

## Heavy $c\bar{c}$ and $b\bar{b}$ quarkonium states and unitarity effects

K. Heikkilä and N. A. Törnqvist

*Department of High Energy Physics, University of Helsinki, 00170 Helsinki 17, Finland*

Seiji Ono\*

*Institut für Theoretische Physik der Rheinisch-Westfälischen Hochschule Aachen, 51 Aachen, West Germany*

(Received 15 February 1983)

We construct a unitarized quarkonium model which uses the quark-pair-creation model for hadronic vertex functions. The mass shifts and mixings induced by  $D\bar{D}$ ,  $F\bar{F}$ ,  $D\bar{D}^*$ , etc., loop diagrams are calculated. These improve in particular the fit to the resonances such as  $\psi(1D)$  and  $\Upsilon(4S)$  which are strongly affected by the first threshold. When comparing the leptonic widths with experiment the unitarized model gives considerably better agreement compared to single-channel  $Q\bar{Q}$  potential models. The improvement is partly because of the mixing between different excitations induced by hadronic loops, and partly because of the fact that the wave functions (at the origin) are modified compared to nonunitarized models.

### I. INTRODUCTION

Since the discovery of  $J/\psi$  and  $\psi'$  in the fall of 1974,<sup>1</sup> eleven charmonium states and at least four  $b$ -quarkonium states have been established. Many authors have explored various potential models to study properties of these states. Some of them are motivated by QCD, but others are not. We have learned that (i) the quarkonium potential is flavor independent (i.e., charmonium and  $b$ -quarkonium states can be described by a common potential), (ii) we can determine the form of the quarkonium potential between 0.1 and 1 fm by studying properties of charmonium and  $b$ -quarkonium states, and (iii) the potential in this region is close to a logarithmic curve.

Although the potential model for  $c\bar{c}$  and  $b\bar{b}$  systems proved to be extremely successful phenomenologically we should not forget that it is not sufficient. Pure potential models fail<sup>2</sup> to predict correct  $e^+e^-$  branching ratios of charmonium states. For example, if the  $S$ - $D$  mixing and recoil effects are neglected,  $\psi(1D)$  cannot decay into  $e^+e^-$  because  $\psi_{1D}(r=0)=0$ , while the experimental datum is<sup>3</sup>

$$\Gamma(\psi(3770) \rightarrow e^+e^-) = 257 \pm 46 \text{ MeV}. \quad (1.1)$$

If one takes into account the  $S$ - $D$  mixing

$$\psi_{1D} = a_{1S}\psi_{1S}^{(0)} + a_{2S}\psi_{2S}^{(0)} + a_{1D}\psi_{1D}^{(0)} + \dots, \quad (1.2)$$

which is induced by the tensor force  $H_T$  in the Breit-Fermi Hamiltonian with a typical quarkonium potential, one finds  $a_{1S} \sim a_{2S} \sim 0.02$ , which is much too small to explain the datum (1.1).

Taking into account the recoil corrections in the matrix elements of the electromagnetic currents, one finds a larger contribution. Then the Van Royen-Weisskopf formula is modified in the following way:

$$\begin{aligned} \Gamma(\psi(1D) \rightarrow e^+e^-) &= 4\alpha^2 e_Q^2 |f_S + f_D|^2 / M_\psi^2, \\ f_S &\equiv a_{1S}\psi_{1S}^{(0)}(0) + a_{2S}\psi_{2S}^{(0)}(0), \\ f_D &\equiv \frac{5}{2\sqrt{2}} a_{1D} \frac{\psi_{1D}^{(0)''}(0)}{m_c^2}. \end{aligned} \quad (1.3)$$

In order to estimate  $\psi_{nS}^{(0)}(0)$  and  $\psi_{1D}^{(0)''}(0)$ , we use a typical potential model<sup>4,5</sup> which describes  $c\bar{c}$  and  $b\bar{b}$  meson masses and even roughly light-meson masses:

$$\begin{aligned} V(R) &= V_0(R) + V_{\text{int}}(R), \\ V_0(R) &= V_{\text{AF}}(R) + aR, \quad V_{\text{int}}(R) = -be^{-R/c}, \\ V_{\text{AF}}(R) &= -\frac{4}{3} \frac{\alpha_s(R)}{R}, \quad \alpha_s(R) = \frac{12\pi}{25} \frac{1}{2 \ln(\mu/R)}, \\ \mu &= (\Lambda e^\gamma)^{-1}, \quad \gamma = 0.5772, \quad \Lambda = 0.5 \text{ GeV}, \\ a &= 0.787 \text{ GeV/fm}, \quad b = 1.378 \text{ GeV}, \quad c = 1.20 \text{ GeV}^{-1}, \\ m_c &= 1.9 \text{ GeV}, \quad m_b = 5.25 \text{ GeV}. \end{aligned} \quad (1.4)$$

We find  $\psi_{1S}(0) = 11.92 \text{ fm}^{-3/2}$ ,  $\psi_{2S}(0) = 9.02 \text{ fm}^{-3/2}$ , and  $\psi_{1D}^{(0)''}(0) = 51.7 \text{ fm}^{-7/2}$ . Therefore,  $f_D \gg f_S$  if the  $S$ - $D$  mixing is induced by the tensor force; thus we neglect  $f_S$ . By using the formula (1.3) one finds

$$\begin{aligned} f_D &= \frac{5}{2\sqrt{2}} \frac{\psi_{1D}^{(0)''}(0)}{m_c^2} = 0.986 \text{ fm}^{-3/2}, \\ \frac{\Gamma_{e\bar{e}}(1D)}{\Gamma_{e\bar{e}}(1S)} &\cong \frac{f_D^2 / M_\psi^2}{\psi_{1S}(0)^2 / M_{J/\psi}^2} \\ &= \frac{(0.986)^2 \times (3.097)^2}{(11.92)^2 \times (3.770)^2} \\ &= \begin{cases} 0.0046 \text{ theory} \\ 0.056 \pm 0.11 \text{ experiment (Ref.3)} \end{cases} \end{aligned} \quad (1.5)$$

Thus this is still too small by an order of magnitude.

Furthermore, looking at the  $e^+e^-$  widths of the radially excited states even more serious problems arise in the naive potential model:

(i)  $\Gamma_{e\bar{e}}(2D)$  is experimentally even larger ( $770 \pm 230 \text{ eV}$ ) than  $\Gamma_{e\bar{e}}(1D)$  ( $257 \pm 46 \text{ MeV}$ ), while the simple potential-model prediction remains small.

(ii) In contrast to this the experimental values of  $\Gamma_{e\bar{e}}(3S)/\Gamma_{e\bar{e}}(1S)$  and  $\Gamma_{e\bar{e}}(4S)/\Gamma_{e\bar{e}}(1S)$  are smaller than

TABLE I. The  $c\bar{c}$  and  $b\bar{b}$  spectra (in MeV) predicted by various potential models.

	Data (Refs. 3,12)	Ono (Refs. 4,5)	Eichten (Ref. 6)	Martin (Ref. 7)	Richardson (Ref. 8)	Buchmüller-Tye (Ref. 9)	Bhanot-Rudaz (Ref. 10)	Krasemann-Ono (Ref. 11)
$\psi(1S)$	3096.9±0.1	3097	3095	3095	3095	3100	3097	3097
$\psi(2S)$	3686.0±0.1	3696	3684	3687	3684	3700	3685	3684
$\psi(3S)$	4030 ±5	4077	4110	4032	4096	4120	4113	4112
$\psi(4S)$	4415 ±6	4393	4460	4280	4440	4480	4483	4483
$\psi(1P)$	3521 <sup>a</sup>	3526	3522	3502	3514	3520	3519	3517
$\psi(1D)$	3770 ±3	3812	3810	3787	3799	3810	3803	3800
$\psi(2D)$	4159 ±20	4152	4190	4092	4173	4190	4191	4189
$\Upsilon(1S)$	9460	9449	9460	9460	9452	9460	9460	9460
$\Upsilon(2S)$	10019	10014	10050	10025	10007	10020	10026	10015
$\Upsilon(3S)$	10351	10343	10400	10360	10338	10350	10339	10328
$\Upsilon(4S)$	10573	10593	10670	10600	10598	10620	10583	10575
$\Upsilon(5S)$		10806	10920	10760	10824	10860	10812	10795
$\Upsilon(6S)$		10999	11140	10920	11025		11014	10997
$\Upsilon(1p)$		9849	9960	9861	9888	9890	9899	9888

<sup>a</sup>Center of gravity.

potential-model predictions.

More systematically, we have studied several potentials which reproduce the  $c\bar{c}$  and  $b\bar{b}$  spectra reasonably well. The mass spectrum and  $\Gamma_{ee}$  are compared with the data in Tables I and II, respectively. We find that predicted values of  $\Gamma_{ee}(3S)/\Gamma_{ee}(1S)$  and  $\Gamma_{ee}(4S)/\Gamma_{ee}(1S)$  are substantially larger (by a factor of two or three) than the data except when using Martin's potential which predicts only a slightly larger value (around one standard deviation). However, Martin's potential predicts too small masses for  $\psi(4S)$  and  $\psi(2D)$ ; thus  $\Gamma_{ee}$  predictions by Martin's potential are unreliable. Therefore, it seems there is no way out for the pure potential model. As we shall show in this paper, many of these difficulties can be overcome when one takes into account the hadronic mass shifts and the mixings induced by the coupling to  $D\bar{D}$ ,  $F\bar{F}$ ,  $D\bar{D}^*$ , etc.

In Sec. II, we show our formalism of the unitarized quark model and the quark-pair-creation model. In Sec. III, the energy shifts, mixing angles, and Okubo-Zweig-Iizuka (OZI) decay widths obtained in our model are shown and the bare mass spectrum is calculated. In Sec. IV we show three potentials which fit the bare mass spectrum.  $e^+e^-$  decay rates are computed and compared

with the data in Sec. V. In Sec. VI, we compare our results with related work. In Sec. VII, a summary and conclusions are presented.

## II. THE UNITARIZED QUARK MODEL AND THE QUARK-PAIR-CREATION MODEL

As widely recognized, because of unitarity, the naive potential model is only an approximation even within a nonrelativistic framework. The  $D\bar{D}$  etc., channels couple strongly to the charmonium giving large widths above the  $D\bar{D}$  threshold. Because of analyticity these channels also contribute large mass shifts both below and above the thresholds in question. Thereby one needs a coupled-channel formalism, where, in addition to a confined channel ( $c\bar{c}$ ), one has several (in this paper,  $D\bar{D}$ ,  $D\bar{D}^* + D^*\bar{D}$ ,  $D^*\bar{D}^*$ ,  $F\bar{F}$ ,  $F\bar{F}^* + F^*\bar{F}$ ,  $F^*\bar{F}^*$ ) two-meson channels (Fig. 1). Calculations within such a formalism are, due to their complexity, found rather sparsely in the literature (Refs. 6 and 13–15 for  $c\bar{c}$  and  $b\bar{b}$ , Refs. 16 and 17 for light quarkonia).

In this paper we use the “unitarized quark model” (UQM) designed by one of us<sup>17</sup> to study mainly  $q\bar{q}$  ( $q = u, d, s$ ) mesons. Combining this model with the

TABLE II. The leptonic widths predicted by various potential models. Unitarity corrections are not taken into account.

	Data (Refs. 3,12)	Ono (Refs. 4,5)	Eichten (Ref. 6)	Martin (Ref. 7)	Richardson (Ref. 8)	Buchmüller-Tye (Ref. 9)	Bhanot-Rudaz (Ref. 10)	Krasemann-Ono (Ref. 11)
$c\bar{c}$								
$\Gamma_{ee}(2S)/\Gamma_{ee}(1S)$	0.45±0.08	0.51	0.44	0.40	0.45	0.46	0.44	0.44
$\Gamma_{ee}(3S)/\Gamma_{ee}(1S)$	0.16±0.04	0.35	0.31	0.25	0.32	0.32	0.33	0.33
$\Gamma_{ee}(4S)/\Gamma_{ee}(1S)$	0.11±0.04	0.27	0.23	0.16	0.24	0.25	0.26	0.28
$b\bar{b}$								
$\Gamma_{ee}(2S)/\Gamma_{ee}(1S)$	0.46±0.03	0.51	0.36	0.51	0.42	0.44	0.43	0.45
$\Gamma_{ee}(3S)/\Gamma_{ee}(1S)$	0.33±0.03	0.36	0.25	0.35	0.30	0.32	0.29	0.31
$\Gamma_{ee}(4S)/\Gamma_{ee}(1S)$	0.23±0.02	0.29	0.20	0.27	0.27	0.26	0.24	0.27
$\Gamma_{ee}(5S)/\Gamma_{ee}(1S)$		0.23	0.18	0.21	0.22	0.25	0.22	0.24
$\Gamma_{ee}(6S)/\Gamma_{ee}(1S)$		0.19	0.16	0.17	0.18		0.20	0.22

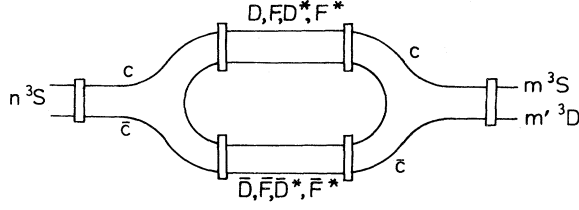


FIG. 1. Coupling of  $c\bar{c}$  states to  $D\bar{D}, F\bar{F}, D\bar{D}^*$ , etc.

quark-pair-creation (QPC) model for the vertex functions ( $\psi \rightarrow D\bar{D}$ , etc.) we have an explicit self-consistent scheme where we can calculate widths, mass shifts, and mixing angles.

The full mass matrix is a sum of a bare term ( $M_{\text{bare}}^2$ ) and a hadronic-mass-renormalization term  $\Pi(s)$ :

$$[M_{n,m}(s)]^2 = (M_{\text{bare},n,m}^2 + \Pi_{n,m}(s)), \quad n, m = 1S, 2S, 1D, \dots \quad (2.1)$$

We use relativistic kinematics, although for heavy  $c\bar{c}$  and  $b\bar{b}$  systems linear mass relations give numerically almost the same results.

The bare-mass term is given by the “naive” single-channel  $c\bar{c}$  potential, while  $\Pi(s)$  contains all the complexities due to the threshold singularities. The imaginary part  $\text{Im}\Pi(s)$  is given by a sum over the thresholds, where each threshold contributes a piece which is a product of two vertex functions  $V_{A,n}^{BC}(s)$ , discussed later, and phase space:

$$\text{Im}\Pi_{nm}^A(s) = \sum_{BC=D\bar{D}, F\bar{F}, \dots} \text{Im}\Pi_{nm}^{ABC}(s), \quad (2.2a)$$

$$\text{Im}\Pi_{nm}^{ABC}(s) = -V_{An}^{BC}(s)V_{Am}^{BC}(s)2\pi E_A E_B k^B \times \theta(s - (m_A + m_B)^2). \quad (2.2b)$$

The kinematic factor  $2\pi E^B E^C$  is introduced for later convenience and  $\theta$  is the step function.

Note that (i) the off-diagonal elements of  $\text{Im}\Pi$  need not be smaller than the diagonal elements (therefore one can obtain comparatively large mixing between the resonances), and (ii) the vertex functions (see below) make  $\text{Im}\Pi$  vanish exponentially for large  $s$ . Therefore one has automatically a cutoff in our model and  $\text{Re}\Pi^A(s)$  can be computed from an unsubtracted dispersion relation

$$\text{Re}\Pi_{nm}^A(s) = -\frac{1}{\pi} \int \frac{\text{Im}\Pi_{nm}(s')}{s-s'} ds'. \quad (2.3)$$

The diagonal elements of  $\text{Re}\Pi(s)$  are in general negative and contribute a negative mass shift to the resonances. In Fig 2(a), we show the real and imaginary parts of  $\Pi_{1S,1S}^{\psi D\bar{D}}(s)$ , i.e., the first diagonal element of the  $D\bar{D}$  contribution to the hadronic mass renormalization. As can be seen, the mass shift term  $\text{Re}\Pi$  is negative below 4.4 GeV. In Fig. 2(b), the corresponding quantities are plotted for the  $1D$ - $1D$  matrix element. For  $2S$ - $2S$  the functions are rather similar to the one for  $1D$ - $1D$ , and for higher radial excitations more nodes appear. The off-diagonal elements are of the same order of magnitude, but for these  $-\text{Im}\Pi(s)$  is not always positive.

Equations (2.1)–(2.3) define the mass matrix in the

reference frame of the bare states. The physical states are obtained after diagonalization:

$$M_{\text{diag}}^2(s) = \alpha^{-1}(s)M^2(s)\alpha(s), \quad (2.4)$$

where the mixing matrix  $\alpha$  satisfies  $\alpha^T\alpha=1$ , i.e.,  $\alpha$  is an orthogonal matrix since  $M^2$  is symmetric. Above the  $D\bar{D}$  threshold,  $\alpha$  obtains an imaginary part, i.e., the mixing matrix becomes complex.

The physical states are given by

$$|n\rangle_{\text{phys}} = \frac{1}{N} \left[ \sum_{n'} \alpha_{nn'}^T |n'\rangle_{\text{bare}} + \int dk a_{D\bar{D}} |D\bar{D}\rangle + \dots \right]. \quad (2.5)$$

The matrix elements of  $\alpha$  determine the relative mixing of the bare states. Since the continuum contributions are small and do not change the results in this paper, we neglect them. Thus our normalization at each resonance energy ( $s=m_R^2$ ) is

$$\sum_m |\alpha_{nm}^T(s=m_R^2)|^2 = 1. \quad (2.6)$$

In principle also the continuum contributions for states below threshold can be computed in our model,

$$\int |a_{D\bar{D}}|^2 dk = \frac{1}{\pi} \int_{s_{\text{th}}}^{\infty} \frac{|\text{Im}\Pi^{\psi D\bar{D}}(s')|}{(m_R^2 - s')^2} ds', \quad (2.7)$$

where  $\Pi^{\psi D\bar{D}}(s)$  denotes the  $D\bar{D}$  contributions in Eq. (2.2) and  $m_{\text{res}}$  is the resonance mass. For a resonance above threshold one cannot define the  $D\bar{D}$  content in this way

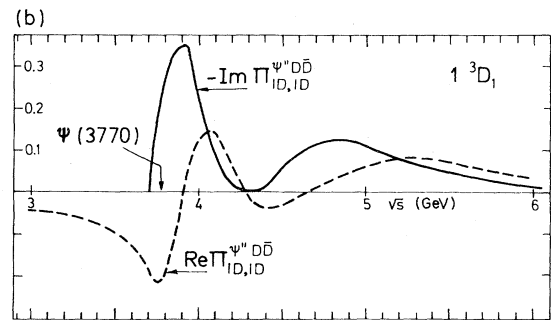
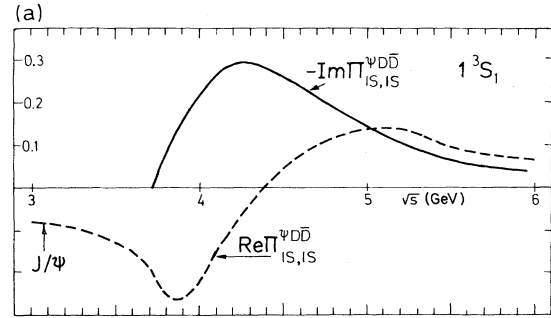


FIG. 2. Real and imaginary parts of a hadronic renormalization term  $\Pi(s)$ .

[Eq. (2.7) diverges], as should be expected for unstable states which eventually go 100% to  $D\bar{D}$ , etc.

To estimate the OZI-rule-allowed coupling and vertex functions of the quarkonia, we use the quark-pair-creation model,<sup>18</sup> since it has proved successful to describe various decay processes. In this model the overlap integral is given by the following matrix element:

$$I_{m_p, m_A}^{L_A} = \gamma_{\text{QPC}} \int d\vec{q} Y_1^{m_p}(2\vec{q} + h_Q \vec{k}) \psi_A^{m_A}(\vec{q} - \frac{1}{2} h_q \vec{k}) \times \psi_B^*(\vec{q}) \psi_C^*(\vec{q}), \quad (2.8)$$

$$h_q = \frac{2m_Q}{m_q + m_Q}, \quad h_Q = \frac{2m_q}{m_q + m_Q}, \quad (2.9)$$

where  $k$  is the decay momentum,  $\gamma_{\text{QPC}}$  is a coupling constant describing the strength of the pair creation, and other notations are self-evident from Fig. 3. It is also possible to define the model so that Eq. (2.8) has an extra phase factor  $(i)^{L_A - L_B - L_C}$  ( $= i^{L_A}$  since  $L_B = L_C$ ). This extra phase factor disappears when the integral is expressed in the spatial coordinate. We choose the phase factor so that we obtain the correct  $e^+e^-$  decay rate of  $\psi(1D)$ .

In order to calculate the overlap integrals, we must assume a potential for the bare meson masses. In principle,

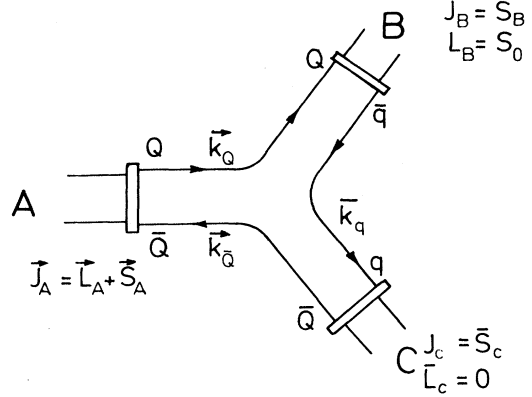


FIG. 3. The  $A$ - $BC$  vertex in QPC.

the bare mass spectrum is determined after unitarity effects have been unfolded. Since hadronic shifts do not depend very sensitively on the details of the potential, we use the potential Eq. (1.8) which was used in previous papers<sup>5,19-22</sup> to compute the overlap integral Eq. (2.8).

The reduced matrix elements are defined for the two allowed angular momenta between final mesons  $L = L_A \pm 1$ :

$$\begin{aligned} \mathcal{L}_{L_A}(-) &\equiv \sum_{m_A, m_p} I_{m_A, m_p}^{L_A} \langle L_A, m_A, 1, m_p | L_A - 1, 0 \rangle \left[ \frac{4\pi}{2L_A - 1} \right]^{1/2} \\ &= -\frac{\gamma_{\text{QPC}}(i)^{L_A}}{\pi} \left[ \frac{6L_A}{2L_A - 1} \right]^{1/2} \\ &\quad \times \int_0^\infty r_A^2 dr_A u_{L_A}(r_A) \int_0^\infty q^2 dq \bar{u}_B(q) \bar{u}_C(q) \left[ -q j_1(qr_A) j_{L_A-1}(\frac{1}{2} h_q kr_A) + \frac{1}{2} h_Q k j_0(qr_A) j_{L_A}(\frac{1}{2} h_q kr_A) \right], \end{aligned} \quad (2.10)$$

$$\begin{aligned} \mathcal{L}_{L_A}(+) &= \sum_{m_A, m_p} I_{m_A, m_p}^{L_A} \langle L_A, m_A, 1, m_p | L_A + 1, 0 \rangle \left[ \frac{4\pi}{2L_A + 3} \right]^{1/2} \\ &= \frac{\gamma_{\text{QPC}}(i)^{L_A}}{\pi} \left[ \frac{6(L_A + 1)}{2L_A + 3} \right]^{1/2} \\ &\quad \times \int_0^\infty r_A^2 dr_A u_{L_A}(r_A) \int_0^\infty q^2 dq \bar{u}_B(q) \bar{u}_C(q) \left[ q j_1(qr_A) j_{L_A+1}(\frac{1}{2} h_q kr_A) + \frac{1}{2} h_Q k j_0(qr_A) j_{L_A}(\frac{1}{2} h_q kr_A) \right]. \end{aligned} \quad (2.11)$$

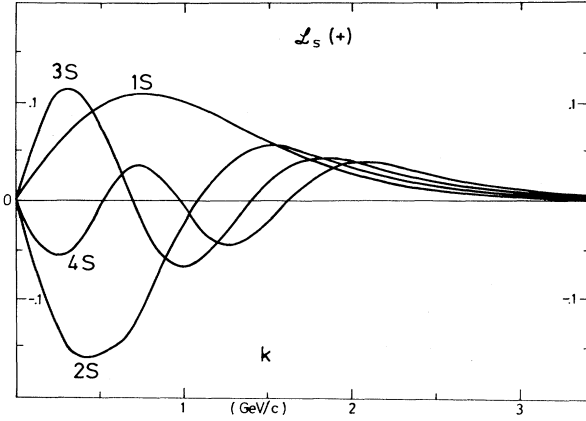
We show forms of  $\mathcal{L}_S(+)$  for  $\psi(1S), \psi(2S), \psi(3S), \psi(4S) \rightarrow D\bar{D}$  and  $\mathcal{L}_D(\pm)$  for  $\psi(1D), \psi(2D), \psi(3D) \rightarrow D\bar{D}$  in Figs. 4 and 5, respectively.

The vertex function for a particular decay  $A \rightarrow BC$  is given by

$$V_A^{BC} = \sum_{S_T, L} \begin{bmatrix} i_Q & i_q & I_B \\ i_Q & i_q & I_C \\ I_A & 0 & I_A \end{bmatrix} \begin{bmatrix} S_Q & S_q & S_B \\ S_Q & S_q & S_C \\ S_A & 1 & S_T \end{bmatrix} \begin{bmatrix} L_A & S_A & J_A \\ 1 & 1 & 0 \\ L & S_T & J_A \end{bmatrix} \epsilon \mathcal{L}(L), \quad (2.12)$$

where

$$\begin{bmatrix} j_1 & j_2 & J_{12} \\ j_3 & j_4 & J_{34} \\ J_{13} & J_{24} & J \end{bmatrix} = [(2J_{12} + 1)(2J_{34} + 1)(2J_{13} + 1)(2J_{24} + 1)]^{1/2} \begin{bmatrix} j_1 & j_2 & J_{12} \\ j_3 & j_4 & J_{34} \\ J_{13} & J_{24} & J \end{bmatrix} \quad (2.13)$$

FIG. 4. The overlap integral  $\mathcal{L}_S(+)$  for  $1S, 2S, 3S, 4S \rightarrow D\bar{D}$ .

$\epsilon = \sqrt{2/3}$  if  $q\bar{q}$  is nonstrange and  $\epsilon = \sqrt{1/3}$  if  $q\bar{q} = s\bar{s}$ ; and  $i_Q, i_q$  ( $S_Q, S_q$ ) is the quark isospin (spin). The amplitudes  $V_A^{BC}$  for  $S$ - and  $D$ -wave  $q\bar{q}$  states are listed in Table III.

If one would neglect the mixing induced by  $\alpha$  in Eq. (2.4), the total width is given by

$$\Gamma_A^{\text{tot}}(s=m_A^2) \approx 2\pi \sum_{\text{thresholds}} |V_A^{BC}(s)|^2 E_B E_C \frac{k^B}{\sqrt{s}}. \quad (2.14)$$

More precisely, in the unitarized model the widths are obtained after diagonalization of  $M^2$  in Eq. (2.4). Then

$$\Gamma_A^{\text{tot}} = -\text{Im} M^2_{\text{diag}}(s)/\sqrt{s} \Big|_{s=m_A^2}, \quad (2.15)$$

and the physical resonance mass is

$$M_A = \text{Re} M^2_{\text{diag}}(s)/\sqrt{s} \Big|_{s=m_A^2}. \quad (2.16)$$

In the same approximation as Eq. (2.14) the mass shift of the resonance  $M_A - M_A^{\text{bare}}$  is given by

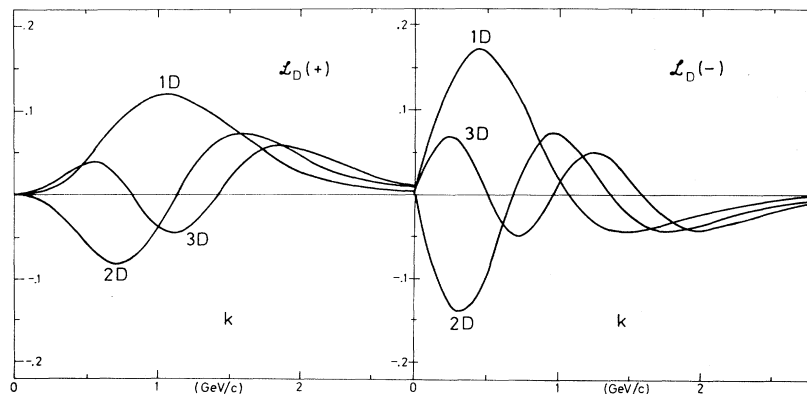
$$\begin{aligned} \Delta_A &= M_A - M_A^{\text{bare}} \\ &\approx \sum_{\text{thresholds}} \text{Re} \Pi^{ABC}(s)/(2\sqrt{s}) \Big|_{s=m_A^2}. \end{aligned} \quad (2.17)$$

TABLE III. Vertex function defined in Eq. (2.12).

Process	$S_T$	$L$	$V/\epsilon$
${}^3D_1 \rightarrow D\bar{D}$ or $F\bar{F}$	0	1	$\frac{1}{2\sqrt{3}} \mathcal{L}_D(-)$
${}^3D_1 \rightarrow D\bar{D}^*$ or $F\bar{F}^*$	1	1	$-\frac{1}{2\sqrt{6}} \mathcal{L}_D(-)$
${}^3D_1 \rightarrow D^*\bar{D}^*$ or $F^*\bar{F}^*$	2	1	$\frac{1}{6\sqrt{5}} \mathcal{L}_D(-)$
	2	3	$\sqrt{7/15} \mathcal{L}_D(+)$
	0	1	$-\frac{1}{6} \mathcal{L}_D(-)$
	0	3	0
${}^3S_1 \rightarrow D\bar{D}$ or $F\bar{F}$	0	1	$\frac{1}{2\sqrt{3}} \mathcal{L}_S(+)$
${}^3S_1 \rightarrow D\bar{D}^*$ or $F\bar{F}^*$	1	1	$\frac{1}{\sqrt{6}} \mathcal{L}_S(+)$
${}^3S_1 \rightarrow D^*\bar{D}^*$	2	1	$\frac{\sqrt{5}}{3} \mathcal{L}_S(+)$
${}^3S_1 \rightarrow D^*\bar{D}^*$	0	1	$-\frac{1}{6} \mathcal{L}_S(+)$
${}^1S_0 \rightarrow D\bar{D}$ or $F\bar{F}$			0
${}^1S_0 \rightarrow D\bar{D}^*$ or $F\bar{F}^*$	1	1	$\frac{1}{2} \mathcal{L}_S(+)$
${}^1S_0 \rightarrow D^*\bar{D}^*$ or $F^*\bar{F}^*$	1	1	$\frac{1}{\sqrt{2}} \mathcal{L}_S(+)$

Each contribution to the mass shift is negative, apart from exceptional cases of a heavy resonance far above the threshold in question [see Figs. 2(a) and 2(b)].

As can be easily verified using Table III our reduced widths near threshold obey well-known ratios:

FIG. 5. Overlap integrals for  $\mathcal{L}_D(+)$  and  $\mathcal{L}_D(-)$  for  $1D, 2D, 3D \rightarrow D\bar{D}$ .

$$\tilde{\Gamma}(^3S_1 \rightarrow D\bar{D}) : \tilde{\Gamma}(^3S_1 \rightarrow D\bar{D}^* + D^*\bar{D}) : \tilde{\Gamma}(^3S_1 \rightarrow D^*\bar{D}^*) : \tilde{\Gamma}(^1S_0 \rightarrow D\bar{D}^* + D^*\bar{D}) : \Gamma(^1S_0 \rightarrow \bar{D}^*\bar{D}^*) = 1:4:7:6:6, \quad (2.18)$$

which follows from the spin-angular-momentum overlaps ( $9-j$  symbols) in Eq. (2.12).

These ratios are, however, obtained in nonrelativistic models only. For example, if one uses Bethe-Salpeter amplitudes one finds these ratios only in the weak-binding limit.

More generally, one starts from the following relativistic amplitudes:

$$T = g_{VPP} \epsilon_{A\mu} (P_B - P_C)^\mu, \quad \text{for } \psi \rightarrow D\bar{D} \text{ (and } \eta_c \rightarrow D\bar{D}^*), \quad (2.19)$$

$$T = g_{VPP} \frac{1}{\sqrt{s}} \epsilon_{\alpha\beta\gamma\delta} P_A^\alpha \epsilon_A^\beta P_C^\gamma \epsilon_C^{*\delta}, \quad \text{for } \psi \rightarrow D\bar{D}^* \text{ (and } \eta_c \rightarrow D^*\bar{D}^*), \quad (2.20)$$

$$\begin{aligned} T = & g_{VVV}^{(1)} (P_A + P_B)_\mu \epsilon_C^{*\mu} \epsilon_A^\nu \epsilon_{B\nu}^* \\ & + g_{VVV}^{(2)} (P_A + P_C)_\mu \epsilon_B^{*\mu} \epsilon_A^\nu \epsilon_{C\nu}^* \\ & + g_{VVV}^{(3)} (P_B - P_C)_\mu \epsilon_A^\mu \epsilon_B^{*\nu} \epsilon_{C\nu}^*, \quad \text{for } \psi \rightarrow D^*\bar{D}^*, \end{aligned} \quad (2.21)$$

and fixes the ratios between the  $g$ 's [in analogy with usual  $SU(6)_W$  arguments, cf. Ref. 19] to give the ratios 1:4:7:6:6 between the reduced widths near threshold.

However, above threshold the helicity amplitudes with a longitudinally polarized  $D^*$  have an additional factor  $s/m_{D^*}^2$ . Of the seven helicity amplitudes in  $\psi \rightarrow D^*\bar{D}^*$ , four have a longitudinally polarized  $D^*$  and in  $\eta_c \rightarrow D^*\bar{D}^*$  and  $D^*$  is always longitudinal. Therefore, one obtains fas-

ter growing widths and instead of 1:4:7:6:6 one finds

$$1:4: \left[ 4 \frac{s}{4m_{D^*}^2} + 3 \right] : 6 \frac{s}{(m_D + m_{D^*})^2} : 6. \quad (2.22)$$

We refer to this as the relativistic spin overlap (RSO) and the previous one as the nonrelativistic spin overlap (NRSO).

For the same reason the RSO gives larger  $\text{Im}\Pi(s)$  for  $\eta_c$  than for  $\psi$ . Neglecting the  $D$ - $D^*$  mass difference one has  $\text{Im}\Pi^{\eta_c} \propto 6 + 6s/4m_{D^*}^2$  vs  $\text{Im}\Pi^\psi \propto 8 + 4s/4m_D^2$ . Therefore also  $\text{Re}\Pi(s)$  in Eq. (2.3) and the negative mass shift will be larger for  $\eta_c$  than for  $\psi$ . This may be a source for the  $\psi$ - $\eta_c$  mass splitting. The difference is numerically non-negligible and we return to this point later.

### III. UNFOLDING THE HADRONIC MASS SHIFTS

We are now turning to the actual comparison with experiment. We compute the mass matrix Eq. (2.1) with the bare masses and pair parameter  $\gamma_{\text{QPC}}$  as free parameters. The eigenvalues are compared with data, whereby  $\gamma_{\text{QPC}}$  is essentially determined by the best-known experimental width. It is known that  $\gamma_{\text{QPC}}$  is fairly flavor independent.<sup>23,24</sup> Therefore, we use the same value  $\gamma_{\text{QPC}} = 3.029$  both for  $c\bar{c}$  and  $b\bar{b}$  states. A similar value of  $\gamma_{\text{QPC}}$  was found<sup>24</sup> from various hadronic decay processes. In Refs. 5, 19, and 10, a slightly different definition of  $\gamma$  was used, i.e.,  $\gamma(\text{Ref. 19}) = (\pi/2\sqrt{6})\gamma_{\text{QPC}}$ .

We show the bare  $c\bar{c}, b\bar{b}$  spectrum in Tables IV and V

TABLE IV. Hadronic mass shifts and the OZI-rule-allowed decay widths (NRSO).

	Physical mass (MeV)	Bare mass (MeV)	$\Delta M$ (MeV)	$\Gamma$ (MeV) experiment (Ref. 3)	$\Gamma$ (MeV) theory
$\psi(1S)$	3096.9	3286.8	-189.9		0
$\psi(2S)$	3686	3837.3	-151.3		0
$\psi(1D)$	3770	3932.1	-162	25±3	10.9
$\psi(3S)$	4030	4127.6	-97.6	52±10	60.1
$\psi(2D)$	4159	4262.3	-103.2	78±20	71.5
$\psi(4S)$	4415	4439.0	-24	43±20	19.6
$\eta_c(1S)$	2981	3167.7	-186.7		0
$\eta_c(2S)$	3599	3728.1	-134.1		0
$\eta_c(3S)$		(4017.0)	-84		72
$\eta_c(4S)$		(4338.0)	-23		29
$\Upsilon(1S)$	9459.7	9489.5	-30		0
$\Upsilon(2S)$	10016	10066	-50		0
$\Upsilon(1D)$	(10130)	(10184)	-54		0
$\Upsilon(3S)$	10347	10409	-62		0
$\Upsilon(2D)$	(10415)	(10469)	-54		0
$\Upsilon(4S)$	10569	10644	-75	14±5	13.9 <sup>a</sup>
$\Upsilon(3D)$	(10650)	(10661)	-11		48.3 <sup>a</sup>
$\Upsilon(5S)$					
$\eta_b(1S)$		(9489.5)	-30		0
$\eta_b(2S)$		(10066)	-50		0
$\eta_b(3S)$		(10409)	-62		0
$\eta_b(4S)$		(10634)	-65		0

<sup>a</sup>Using the recently reported experimental  $B$ -meson mass (Ref. 39) (instead of our guess of 5280 MeV), the  $\Upsilon(4S)$  width increases to 19.8 MeV and  $\Upsilon(3D)$  decreases (because of the node structure) to 40 MeV.

TABLE V. Same as Table IV, but with RSO.

	Bare mass (MeV)	$\Delta M$ (MeV)	$\Gamma$ (MeV) theory
$\psi(1S)$	3309.3	-212.4	0
$\psi(2S)$	3851.8	-166	0
$\psi(1D)$	3932.1	-162	11
$\psi(3S)$	4136.5	-106.5	62.4
$\psi(2D)$	4262.1	-103	71.1
$\psi(4S)$	4441.6	-26.6	21.6
$\eta_c(1S)$	3204.2	-223	0
$\eta_c(2S)$	3751.5	-152.5	0
$\eta_c(3S)$	(4032.5)	-102.5	78
$\eta_c(4S)$	(4343.6)	-28.6	32

by using RSO and NRSO, respectively. The results are rather insensitive to the number of radial excitations included. Only the highest state depends, as expected, slightly on whether or not the following radial excitation is included.

As can be seen, the bare masses are all heavier by 20–200 MeV than the physical masses due to the generally negative sign of mass shifts as discussed in Sec. II. But the mass shifts are not equal in magnitude, e.g., the  $\psi(1S)$  state is shifted more than the higher excitations. This is because the node structure in a higher excitation suppresses the mass shifts. On the other hand, the larger distance to the thresholds for 1S compared to 2S compensates for this effect somewhat.

The mass shifts for the  $b$ -quarkonium states are quite different from those of charmonium because the position of the  $B\bar{B}, B\bar{B}^*$ , etc. thresholds are relatively much higher (near the 4S state rather than 2S for charmonium). Therefore the lowest  $\Upsilon$  states have the smallest mass shift.

The mass shift for  $n^3S$  is not much different from that for  $n^1S$ . For NRSO this is understandable from Eq. (2.18). For the RSO [Eq. (2.22)] the mass shift of the  $\eta_c$  is slightly larger than that of the  $\psi$ , i.e., part of the  $\psi$ - $\eta_c$  splitting could be accounted for by the hadronic shifts. In general, hadronic mass shifts between different  $J^{PC}$  states are sensitive to assumptions of the spin symmetry assumed. For example, with fairly small violation of the ratios in Eq. (2.18), a larger contribution to the  $\psi$ - $\eta_c$  mass splitting could be obtained. But, assuming Eq. (2.18), the only difference comes from mass difference between  $D$  and  $D^*$  and that between  $F$  and  $F^*$ . Experimentally known hyperfine splittings are

$$\Delta M = M(J/\psi) - M(\eta_c) = 116 \pm 4 \text{ MeV (Ref. 25) ,}$$

$$\Delta M^* = M(\psi') - M(\eta_c') = 93 \pm 5 \text{ MeV (Refs. 25 and 26) ,}$$

i.e.,

$$\Delta M^* / \Delta M = 0.80 \pm 0.03 ,$$

Unfolding unitarity effects we get hyperfine splitting for the bare states (see Tables IV and V):

For NRSO:

$$\Delta M(\text{bare}) = \Delta M + 3 \text{ MeV} = 119 \text{ MeV} ,$$

$$\Delta M^*(\text{bare}) = \Delta M^* + 17 \text{ MeV} = 110 \text{ MeV} , \quad (3.2)$$

i.e.,

$$\Delta M^*(\text{bare}) / \Delta M(\text{bare}) = 0.92 .$$

For RSO:

$$\Delta M(\text{bare}) = \Delta M - 11 \text{ MeV} = 102 \text{ MeV} ,$$

$$\Delta M^*(\text{bare}) = \Delta M^* + 14 \text{ MeV} = 107 \text{ MeV} , \quad (3.3)$$

i.e.,

$$\Delta M^*(\text{bare}) / \Delta M(\text{bare}) = 1.05 .$$

From a potential model we can compute  $\Delta M^* / \Delta M$  by using the Breit-Fermi Hamiltonian.  $\Delta M^* / \Delta M$  becomes slightly larger if a simple contact term  $H_{ss} \propto \delta^3(\vec{r}) \vec{\sigma}_1 \cdot \vec{\sigma}_2$  is used than the one obtained by assuming  $H_{ss} \propto \nabla^2 V$ . In any case,  $\Delta M^* / \Delta M$  stays around 0.5. Therefore, we confirm the conclusion by Martin and Richard,<sup>27</sup> i.e., if we take into account the effect of virtual  $D$ -meson pairs the ratio  $\Delta M^* / \Delta M$  becomes difficult to accommodate by a potential model.

As seen in Table I if the unitarity effect is not unfolded the potential model usually predicts too high a value for  $\Upsilon(4S)$ . This is why it is generally believed that the  $\Upsilon(4S)$  mass is strongly influenced by the  $B\bar{B}$  threshold. Our calculation indeed gives such a large shift for  $\Upsilon(4S)$  (see Table IV) which makes the fit by a potential model easier.

In Tables IV and V, OZI-rule-allowed decay widths are also listed. Agreement with the data is reasonably good. We have fixed the  $B$ -meson mass so that  $\Upsilon'''$  has correct decay width. We use the potential of Eq. (1.4) to fix mass differences  $B^* - B$ ,  $B_s - B$ , and  $B_s^* - B$ . Thus we use  $B = 5280 \text{ MeV}$ ,  $B^* = 5325 \text{ MeV}$ ,  $B_s = 5362 \text{ MeV}$ , and  $B_s^* = 5398 \text{ MeV}$ . See, however, Ref. 28.

The QPC without mixing predicts<sup>19,29</sup> the correct ( $\sim 22 \text{ MeV}$ ) decay width for  $\psi(1D)$  while we obtain here only 11 MeV. We indeed get 19 MeV before mixing. However, due to the strong mixing with  $\psi(2S)$ , the  $\psi(1D)$  state tends to decouple with  $D\bar{D}$ , while the  $\psi(2S)$ - $D\bar{D}$  coupling becomes stronger. In general, if two energy levels which are close to each other couple to a certain channel, the higher one decouples and the lower one couples stronger after the mixing (see Ref. 30).

#### IV. POTENTIAL MODELS WHICH FIT BARE MASS SPECTRA

In the previous sections we have computed mass shifts due to virtual annihilation into two meson states. After removing these mass shifts we find a new spectrum which we call the bare-mass spectrum. The bare mass spectrum is higher than the physical mass spectrum by 20–200 MeV for  $c\bar{c}$  states and by around 50 MeV higher for  $b\bar{b}$ .

Any spectrum predicted by a model (potential model, field-theoretical model, etc.) which neglects these loop corrections should be compared to the bare spectrum rather than to the physical spectrum. In the following we try to find potential models which fit the bare mass spectrum.

We consider three potentials:

(1) Martin potential<sup>7</sup>:

$$\begin{aligned}
V(R) &= -7.873 + 6.870R^{0.100}, \\
m_c &= 1.8 \text{ GeV}, m_b = 5.10 \text{ GeV}, \\
[V(R) \text{ and } R^{-1} \text{ in GeV}].
\end{aligned}
\tag{4.1}$$

(2)  $R^{2/3}$  + Coulomb potential:

$$\begin{aligned}
V(R) &= -\frac{4}{3} \frac{\alpha_s}{R} + BR^{2/3} - A \\
A &= 980 \text{ MeV}, m_c = 1.90 \text{ GeV}, \\
B &= 0.35, m_b = 5.215 \text{ GeV}, \\
\alpha_s &= 0.35.
\end{aligned}
\tag{4.2}$$

(3) Lichtenberg-Wills (LW) potential<sup>31,32</sup>:

$$\begin{aligned}
V(R) &= \frac{8\pi}{25} \frac{(1-\lambda R)^2}{R \ln(\lambda R)} + A, \\
\lambda &= \Lambda e^\gamma, \gamma = 0.5772 \dots \text{ (Euler's const.)}, \\
\Lambda &= 350 \text{ MeV}, m_c = 1.90 \text{ GeV}, \\
A &= -850 \text{ MeV}, m_b = 5.21 \text{ GeV}.
\end{aligned}
\tag{4.3}$$

These three potentials are almost numerically identical between 0.1 and 1.5 fm. However, at short range ( $< 0.1$  fm) they have very different behaviors:

$$V(R) \xrightarrow{R \rightarrow 0} \begin{cases} \text{constant, Martin potential,} \\ -\frac{4\alpha_s}{3} \frac{1}{R}, R^{2/3} + \text{Coulomb potential,} \\ \frac{8\pi}{25} \frac{1}{R \ln(\lambda R)}, \text{ LW potential.} \end{cases}$$

At origin the Martin potential is not singular, while the second one has a  $1/R$  singularity and the LW potential has a softer singularity.

As seen from Table VI, these three potentials reproduce the bare-mass spectra of  $c\bar{c}$  and  $b\bar{b}$  reasonably well. We have changed the potential parameters and the quark masses from the original values. Lichtenberg and Wills<sup>32</sup> used  $\Lambda = 676$  MeV, but after unfolding unitarity effects we find  $\Lambda = 350$  MeV.

As for the quark mass difference  $m_b - m_c$ , we find around 3.31 GeV for all three potentials. By using the Feynman-Hellmann theorem one can determine  $m_b - m_c$  in a potential-independent way. By neglecting the spin-dependent force, Bertlmann and Martin<sup>33</sup> found  $3.36 < m_b - m_c < 3.69$  GeV and by taking into account the spin-dependent force, Bertlmann and Ono<sup>34</sup> found  $3.30 < m_b - m_c < 3.55$  GeV. Our value for  $m_b - m_c$  is

TABLE VI. Comparison between the bare mass spectrum and the potential-model predictions (MeV).

$c\bar{c}$	Bare mass	$R^{2/3}$ + Coulomb	Martin	Lichtenberg-	
				Wills	
1S	3287	3283	3258	3245	
2S	3837	3820	3861	3803	
1D	3932	3938	3979	3916	
3S	4128	4165	4212	4168	
2D	4260	4242	4283	4242	
4S	4439	4438	4464	4461	
1P		3686	3694	3649	
$b\bar{b}$					
1S	9489	9513	9494	9510	
2S	10066	10082	10067	10051	
1D		10229	10180	10176	
3S	10409	10391	10402	10369	
2D		10483	10469	10448	
4S	10644	10623	10641	10612	
1P		9991	9908	9931	
2P		10317	10290	10275	

below these lower bounds of Ref. 33. This is understandable because if one unfolds the unitarity effects, quark mass differences become smaller. This is related to the fact that lighter quarkonium states shift downward more than heavier ones.

## V. MIXINGS AND $e^+e^-$ DECAY RATES OF QUARKONIA

The mixings of various states are given by

$$\psi_i = \sum_j \alpha_{ij}^T \psi_j^{(0)}, \quad i, j = \begin{cases} 1S, 2S, 1D, 3S, 2D, 4S \text{ for } c\bar{c} \\ 1S, 2S, 1D, 3S, 2D, 4S, 3D \text{ for } b\bar{b} \end{cases}
\tag{5.1}$$

$\alpha_{i,j}^T$  for  $c\bar{c}$  and  $b\bar{b}$  are listed in Tables VII and VIII, respectively.

Normalization of these states is given in (2.6). As expected, mixings 2S-1D, 3S-2D, and 4S-3D are larger than other mixings because these masses are close to each other. The  $e^+e^-$  decay rates of quarkonia are given by Eq. (1.3), where

$$|f_S + f_D|^2 \equiv \left| \sum_{k=S \text{ states}} \alpha_{ik}^T \psi_k^{(0)}(0) + \frac{5}{2\sqrt{2}m_Q^2} \sum_{k=D \text{ states}} \alpha_{ik}^T \psi_k^{(0)'}(0) \right|^2.
\tag{5.2}$$

TABLE VII. Mixing coefficients  $\alpha_{ij}^T$  defined in Eq. (5.1) for  $c\bar{c}$  states.

	1S		2S		1D		3S		2D		4S	
	Re	Im	Re	Im	Re	Im	Re	Im	Re	Im	Re	Im
$\psi(1S)$	0.9997	0	0.0128	0	-0.0002	0	-0.0127	0	0.0005	0	-0.0137	0
$\psi(2S)$	0.0276	0	0.9883	0	-0.1480	0	0.0179	0	-0.0055	0	-0.0180	0
$\psi(1D)$	-0.0028	-0.0010	0.2061	0.0670	0.9747	-0.0139	0.0169	0.0179	0.0444	-0.0157	-0.0030	-0.0049
$\psi(3S)$	0.0310	-0.0134	0.0283	0.0981	-0.0161	0.0299	0.9867	0.0006	-0.1118	0.0210	0.0028	-0.0292
$\psi(2D)$	0.0125	0.0080	-0.0450	-0.0290	-0.0388	0.0376	0.0854	0.1509	0.9813	-0.0129	-0.0092	0.0259
$\psi(4S)$	0.0510	-0.0176	0.0478	0.0365	-0.0016	-0.0024	-0.1340	0.0129	0.0038	-0.0079	0.9875	0.0009

TABLE VIII. Same as Table VII but for  $b\bar{b}$  states.

	1S		2S		1D		3S		2D		4S		3D	
	Re	Im												
$\Upsilon(1S)$	0.9995	0	-0.0298	0	0.0022	0	-0.0103	0	0.0008	0	-0.0019	0	0.0001	0
$\Upsilon(2S)$	0.0481	0	0.9966	0	-0.0387	0	-0.0518	0	0.0066	0	-0.0145	0	0.0024	0
$\Upsilon(1D)$	-0.0017	0	0.0458	0	0.996	0	0.0068	0	-0.0726	0	0.0006	0	-0.0245	0
$\Upsilon(3S)$	0.0211	0	0.0926	0	-0.0233	0	0.9909	0	-0.0813	0	-0.0421	0	0.0090	0
$\Upsilon(2D)$	-0.0001	0	0.0015	0	0.1164	0	0.0966	0	0.9856	0	0.0060	0	-0.0755	0
$\Upsilon(4S)$	0.0078	0.0006	0.0174	-0.0024	-0.0154	-0.0022	0.1609	0.0148	-0.1371	-0.0583	0.8987	-0.0489	-0.3641	-0.0926
$\Upsilon(3D)$	0.0045	-0.0029	-0.0275	0.101	0.0522	-0.0389	0.0519	-0.0287	-0.0534	0.1524	-0.2326	-0.0582	0.9528	-0.0017

The wave functions  $\psi_k^{(0)}$  must be determined by using a potential which reproduces the bare mass spectrum. We use the three potentials discussed in the previous section. Results are compared with the data in Table IX. Compared to Table II, we find remarkable improvements in  $\Gamma_{e\bar{e}}(3S)/\Gamma_{e\bar{e}}(1S)$ ,  $\Gamma_{e\bar{e}}(4S)/\Gamma_{e\bar{e}}(1S)$ , and  $\Gamma_{e\bar{e}}(1D)/\Gamma_{e\bar{e}}(1S)$ . The increase of  $\Gamma_{e\bar{e}}(1D)$  and  $\Gamma_{e\bar{e}}(2D)$  comes from the  $S$ - $D$  mixing and the decrease of  $\Gamma_{e\bar{e}}(3S)$  and  $\Gamma_{e\bar{e}}(4S)$  partly comes from the  $S$ - $D$  mixing and partly come from the potential behavior for large  $r$  (since these potentials increase slower than linearly, the wave functions of higher states spread out).

We find no way to accommodate the extraordinarily large branching ratio

$$\Gamma_{e\bar{e}}(2D) = 770 \pm 230 \text{ keV}, \quad (5.3)$$

although our prediction is much larger than those of potential models. The datum (5.3) is 12 times higher than our prediction.

To clarify the situation consider  $2D$  and  $3S$  states only, and neglect mixings with the other states:

$$\psi(3S) = \cos\theta \psi_{3S}^{(0)} - \sin\theta \psi_{2D}^{(0)}, \quad (5.4)$$

$$\psi(2D) = \sin\theta \psi_{3S}^{(0)} + \cos\theta \psi_{2D}^{(0)}.$$

From Eq. (1.3) one gets

$$\frac{\Gamma_{e\bar{e}}(2D)}{\Gamma_{e\bar{e}}(3S)} = \frac{\left| \sin\theta \psi_{3S}^{(0)}(0) + \cos\theta \frac{5}{2\sqrt{2}m_c^2} \psi_{2D}^{(0)''}(0) \right|^2}{\left| \cos\theta \psi_{3S}^{(0)}(0) - \sin\theta \frac{5}{2\sqrt{2}m_c^2} \psi_{2D}^{(0)''}(0) \right|^2}. \quad (5.5)$$

In a typical potential model one gets

$$\frac{|\psi_{3S}^{(0)}(0)|}{\frac{5}{2\sqrt{2}m_c^2} |\psi_{2D}^{(0)''}(0)|} \sim 8. \quad (5.6)$$

By neglecting the second term for simplicity one obtains

$$\frac{\Gamma_{e\bar{e}}(2D)}{\Gamma_{e\bar{e}}(3S)} = \tan^2\theta. \quad (5.7)$$

Experimentally this is of order one. This means  $\theta \sim 45^\circ$ , thus  $3S$  and  $2D$  are nearly equally mixed. In such a case,  $\Gamma_{e\bar{e}}(3S)$  must be around one half ( $\sin^2 45^\circ = \frac{1}{2}$ ) of the one predicted by the potential model. From Table III, one finds that this might be the case.

However, it is difficult to find such a large  $S$ - $D$  mixing within the model which we are considering here.

## VI. COMPARISON WITH RELATED WORKS

Mass shifts of  $c\bar{c}$  and  $b\bar{b}$  states due to the virtual annihilation into two meson have been studied comprehensively by the Cornell group<sup>6,13</sup> and the Nijmegen group.<sup>14</sup> The Nijmegen group uses a harmonic-oscillator potential and QPC, while the Cornell group uses a Coulomb-plus-linear-type potential with a different kind of coupled-

TABLE IX. Same as Table II, but unitarity corrections are taken into account.

$c\bar{c}$	Data	$R^{2/3} + \text{Coulomb}$	Martin	Lichtenberg- Wills
$\Gamma_{ee}(2S)/\Gamma_{ee}(1S)$	$0.45 \pm 0.08$	0.351	0.348	0.373
$\Gamma_{ee}(3S)/\Gamma_{ee}(1S)$	$0.16 \pm 0.04$	0.247	0.227	0.269
$\Gamma_{ee}(4S)/\Gamma_{ee}(1S)$	$0.11 \pm 0.04$	0.154	0.133	0.171
$\Gamma_{ee}(1D)/\Gamma_{ee}(1S)$	$0.050 \pm 0.011$	0.0311	0.0386	0.0362
$\Gamma_{ee}(2D)/\Gamma_{ee}(1S)$	$0.17 \pm 0.06$	0.0108	0.0129	0.0133
$b\bar{b}$				
$\Gamma_{ee}(2S)/\Gamma_{ee}(1S)$	$0.46 \pm 0.03$	0.378	0.534	0.464
$\Gamma_{ee}(3S)/\Gamma_{ee}(1S)$	$0.33 \pm 0.03$	0.293	0.4287	0.379
$\Gamma_{ee}(4S)/\Gamma_{ee}(1S)$	$0.23 \pm 0.02$	0.240	0.3550	0.325
$\Gamma_{ee}(1D)/\Gamma_{ee}(1S)$		0.000 272	0.000 137	0.000 253
$\Gamma_{ee}(2D)/\Gamma_{ee}(1S)$	$< 0.04$	0.0010	0.000 808	0.001 06
$\Gamma_{ee}(3D)/\Gamma_{ee}(1S)$		0.0127	0.0210	0.0183

channel model.

We believe that our model has various advantages.

(i) We use the QPC which is already confirmed to be able to explain various hadronic decay processes (e.g., see Refs. 18–22, 24, 29, and 35–37).

(ii) We are using QCD-motivated potentials consistently. We have shown three potentials which fit the bare-mass spectra for  $c\bar{c}$  and  $b\bar{b}$ . The Cornell group used a Coulomb-plus-linear potential only for  $c\bar{c}$  and a harmonic-oscillator potential for the  $D, D^*$  meson.

Compared to the Cornell results our mass shifts for  $c\bar{c}$  states are of the same order of magnitude, but relative shifts are different. The Cornell group found only  $-48$  MeV for the  $c\bar{c} 1^3S_1$  state while our value is  $-190$  MeV. The Nijmegen group also found that the mass shift for  $1S$  states is large in agreement with our result. It has been argued<sup>38</sup> that the mass shift of states much below threshold is small; thus the virtual  $DD\bar{D}$  can survive only  $\Delta t \sim 1/600$  MeV  $\sim 0.3$  fm, which is shorter than the size of the  $D$  meson ( $\sim 0.6$  fm). In our model this effect is included in the energy denominator of Eq. (2.3), which suppresses the mass shift for states far below the  $DD\bar{D}$  threshold [cf. Fig. 2(a), ReII].

The Cornell group did not chose their potential parameters very carefully. From Table VII of Ref. 11, we see that they predict correct  $1^3S_1, 2^3S_1$ , and  $1P$  states, while they got  $M(4^3S_1) = 4625$  MeV, this is as much as 210 MeV higher than the experimental value 4415. Another problem is that they found  $2^3D_1 - 3^3S_1 = 5$  MeV, while the experimental value is  $129 \pm 25$  MeV. Our potential parameters are chosen much more carefully (see Table VIII).

As to the  $\psi(3770)$ , our results are different from theirs:

	Cornell results	Our results	Experiment <sup>3</sup>
$\Gamma_{\text{tot}}$	30 MeV	11 MeV	$25 \pm 3$ MeV
$\frac{\Gamma_{ee}(1D)}{\Gamma_{ee}(1S)}$	0.0149	0.03–0.04	$0.056 \pm 0.011$

Thus these widths are sensitive to the details of the model.

As to the  $2D$  state, we agree with the conclusion of the Cornell group, i.e., we find too small a mixing with the  $3^3S_1$  state.

One might think that the  $DD\bar{D}_p$  thresholds ( $D_p = \bar{u}c$ ,  $P$  state,  $D_p \sim 2400$  MeV) become important. However, in calculation of the overlap integral the integration of a function which includes the radial wave function  $R_{4s}(r)$  becomes small due to the node structure of  $R_{4s}(r)$ . Thus mass shifts due to  $DD_p$  thresholds should be relatively small. On the other hand, the mass shift for the  $1S$  state due to the  $D_p$  state becomes also relatively small because of the large distance. Therefore, we expect relatively small negative shifts due to  $DD_p$  thresholds for the  $\psi(1S), \dots, \psi(4S)$  states.

For the  $Y$  states the corresponding  $B\bar{B}_p$  thresholds are very far away at about 11.1 GeV and therefore the contribution from these should be very small.

## VII. SUMMARY AND CONCLUSIONS

We have combined the unitarized quark model with the quark-pair-creation model and studied OZI-rule-allowed two-meson couplings to  $c\bar{c}$  and  $b\bar{b}$  states. Our conclusions are as follows.

(i) Hadronic mass shifts due to the coupling to virtual mesons are from  $-20$  to  $-200$  MeV for  $c\bar{c}$  and around  $-50$  MeV for  $b\bar{b}$ . We have studied several potential models which fit the bare-mass spectra of  $c\bar{c}$  and  $b\bar{b}$  obtained after unfolding the mass shifts. The Lichtenberg and Wills potential is one of them, where we need  $\Lambda = 350$  MeV to fit the bare mass spectra while Lichtenberg and Wills used  $\Lambda = 676$  MeV to fit the physical spectra. Experimentally  $\Lambda_{\overline{MS}} = 50-400$  MeV (where  $\overline{MS}$  denotes the modified minimal-subtraction scheme).

(ii) We need a smaller quark mass difference  $m_b - m_c$  to fit the bare-mass spectra than that to fit the physical mass spectra.

(iii) Our value of  $\Gamma(1^3D_1 \rightarrow e^+e^-)$  is much nearer to the datum than that of a coupled-channel model by the Cornell group. We have obtained much improved values

of  $\Gamma(\psi \rightarrow e^+e^-)$  for higher excited  $c\bar{c}$  states compared to the pure potential model. This is partly due to the mixing induced by the matrix  $\alpha$  and partly due to the fact that the potential for the bare states is modified giving broader wave functions for higher states and therefore smaller  $\psi(0)$ . As for the  $2D$  state,  $\Gamma_{e^+e^-}$  becomes too small in agreement with the Cornell model.

(iv) Our model nicely reproduces the spectra, OZI-rule-allowed decay widths, and  $\Gamma_{e^+e^-}$  for  $c\bar{c}$  and  $b\bar{b}$  states which include even the one for which the Cornell model calculation completely breaks down, i.e., the  $4S$   $c\bar{c}$  state.

(v) As for the ratio

$$\Delta M^*/\Delta M = [M(\psi') - M(\eta'_c)] / [M(J/\psi) - M(\eta_c)] ,$$

we have reached the same conclusion as Martin and Richard,<sup>27</sup> i.e.,  $\Delta M^*/\Delta M$  for the bare mass spectra is difficult to explain by a potential model and even the unitarization does not help in this case if one believes Eq. (2.18).

(vi) For  $b$ -quarkonium states we find the largest mass

shift for  $\Upsilon(4S)$  because the  $B\bar{B}$  threshold is near this resonance. Such a large shift to  $\Upsilon(4S)$  makes the fit by a potential model easier. The  $b$ -quarkonium mass shifts are rather different than those of charmonium because of the different relative position of the thresholds ( $B\bar{B}, B\bar{B}^*$ , etc. are near the  $4S$  state) compared to the charmonium case ( $D\bar{D}, D\bar{D}^*$ , etc. are just above the  $2S$  state). Therefore the mass shift of the lowest  $\Upsilon$  state is the smallest.

#### ACKNOWLEDGMENTS

We would like to thank E. van Beveren, J. Ellis, H. Krasemann, A. Le Yaouanc, A. Martin, O. Pene, J.-M. Richard, M. Roos, and P. M. Zerwas for discussions. One of us (S.O.) is grateful for the financial support of the Bundesministerium für Forschung und Technologie and of the Research Institute for Theoretical Physics in Helsinki where this work was finished. He also would like to thank the High Energy Physics Group in Helsinki for its hospitality.

\* Present address: Laboratoire de Physique Théorique et Hautes Energies, Orsay, France.

<sup>1</sup>J. J. Aubert *et al.*, Phys. Rev. Lett. **33**, 1404 (1974); J. E. Augustin *et al.*, *ibid.* **33**, 1406 (1974); G. S. Abrams *et al.*, *ibid.* **33**, 1453 (1974).

<sup>2</sup>J.-M. Richard, Z. Phys. C **4**, 211 (1980).

<sup>3</sup>Particle Data Group, M. Roos *et al.*, Phys. Lett. **111B**, 1 (1982).

<sup>4</sup>S. Ono, Phys. Rev. D **20**, 2975 (1979).

<sup>5</sup>S. Ono, Z. Phys. C **8**, 7 (1981).

<sup>6</sup>E. Eichten, K. Gottfried, T. Kinoshita, K. D. Lane, and T.-M. Yan, Phys. Rev. D **17**, 3090 (1978); **21**, 313(E) (1980).

<sup>7</sup>A. Martin, Phys. Lett. **100B**, 511 (1981).

<sup>8</sup>L. Richardson, Phys. Lett. **82B**, 272 (1979).

<sup>9</sup>W. Buchmüller and S.-H.H. Tye, Phys. Rev. D **24**, 132 (1981).

<sup>10</sup>G. Bhanot and S. Rudaz, Phys. Lett. **78B**, 119 (1978).

<sup>11</sup>H. Krasemann and S. Ono, Nucl. Phys. **B154**, 283 (1979).

<sup>12</sup>R. D. Schamberger, in *Proceedings of the 1981 International Symposium on Lepton and Photon Interactions at High Energies, Bonn*, edited by W. Pfeil (Physikalisches Institut, Universität Bonn, Bonn, 1981).

<sup>13</sup>E. Eichten, K. Gottfried, T. Kinoshita, K. D. Lane, and T.-M. Yan, Phys. Rev. D **21**, 203 (1980).

<sup>14</sup>E. van Beveren, C. Dullemond, and G. Rupp, Phys. Rev. D **21**, 772 (1980); E. van Beveren, Z. Phys. C **17**, 135 (1983); E. van Beveren, G. Rupp, T. A. Rijken, and C. Dullemond, Phys. Rev. D **27**, 1527 (1983).

<sup>15</sup>S. Jacobs, K. J. Miller, and M. G. Olsson, Phys. Rev. Lett. **50**, 1181 (1983).

<sup>16</sup>G. Fogli and G. Preparata, Nuovo Cimento **48A**, 235 (1978); A. C. A. Maciel and J. Paton, Nucl. Phys. **B181**, 277 (1981).

<sup>17</sup>N. A. Törnqvist, Ann. Phys. (N.Y.) **135**, 1 (1978); M. Roos and N. A. Törnqvist, Z. Phys. C **5**, 205 (1980); N. Törnqvist, Phys. Rev. Lett. **49**, 624 (1982); Nucl. Phys. **B203**, 268 (1982).

<sup>18</sup>A. Le Yaouanc, L. Oliver, O. Pene, and J.-C. Raynal, Phys. Rev. D **8**, 2223 (1973).

<sup>19</sup>S. Ono, Phys. Rev. D **23**, 1118 (1981).

<sup>20</sup>I. I. Bigi and S. Ono, Nucl. Phys. **B189**, 229 (1981).

<sup>21</sup>S. Ono, Phys. Rev. D **26**, 3266 (1982).

<sup>22</sup>S. Ono and O. Pene, Report No. LP THE Orsay, 82/36 (unpublished).

<sup>23</sup>M. Chaichian and R. Kögerler, Ann. Phys. (N.Y.) **124**, 61 (1980).

<sup>24</sup>J. P. Ader, B. Bonnier, and S. Sood, Nuovo Cimento **68A**, 1 (1982).

<sup>25</sup>C. Edwards *et al.*, Phys. Rev. Lett. **48**, 70 (1982).

<sup>26</sup>D. L. Scharre, in *Proceedings of the 1981 International Symposium on Lepton and Photon Interactions at High Energies, Bonn* (Ref. 12).

<sup>27</sup>A. Martin and J.-M. Richard, Phys. Lett. **115B**, 323 (1982).

<sup>28</sup>After this work was finished the CLEO group at Cornell measured the  $B^+$  and  $B^0$  masses to be 5270.7 and 5374.2 MeV. Our results do not change when these masses are used, except for the  $\Upsilon(4S)$  width and mass shift, which increases somewhat.

<sup>29</sup>A. Le Yaouanc, L. Oliver, O. Pene, and J.-C. Raynal, Phys. Lett. **72B**, 57 (1977).

<sup>30</sup>N. A. Törnqvist, Lett. Nuovo Cimento **46A**, 633 (1978); Phys. Lett. **69B**, 193 (1977).

<sup>31</sup>D. B. Lichtenberg and J. G. Wills, Nuovo Cimento **47A**, 483 (1978).

<sup>32</sup>G. Fogleman, D. B. Lichtenberg, and J. G. Wills, Lett. Nuovo Cimento **26**, 369 (1979).

<sup>33</sup>R. A. Bertlmann and A. Martin, Nucl. Phys. **B168**, 111 (1980).

<sup>34</sup>R. A. Bertlmann and S. Ono, Z. Phys. C **10**, 37 (1981).

<sup>35</sup>A. Le Yaouanc, L. Oliver, O. Pene, and J.-C. Raynal, Phys. Rev. D **8**, 2223 (1973).

<sup>36</sup>W. B. Kaufmann and R. J. Jacob, Phys. Rev. D **10**, 1051 (1974).

<sup>37</sup>A. Bradly and D. Robson, Z. Phys. C **4**, 67 (1980).

<sup>38</sup>P. M. Zerwas (private communication).